Fizyka Nyzkykh Temperatur/Low Temperature Physics, 2026, Vol. 52, No. 10, pp. 1363–1370

Elasto-optic properties of K_2SO_4 crystals

O. A. Markevych[1], O. M. Horina[2], V. Y. Stadnyk[1]*, R. S. Brezvin[1], Z. O. Kohut[3], and I. B. Pirko[4]

[1]*Ivan Franko National University of Lviv, Lviv 79005, Ukraine*

[2]*Lviv State University of Life Safety, Lviv 79000, Ukraine*

[3]*Czestochowa University of Technology, Częstochowa 42-201, Poland*

[4]*Ukrainian National Forestry University, Lviv 79057, Ukraine*

*E-mail: vasylstadnyk@ukr.net

Received March 11, 2026, revised May 11, 2026, advance online published August 20, 2026

The elastic stiffness coefficients of K_2SO_4 crystals at room temperature were calculated. The coefficient C_{66} is the smallest among the diagonal components, indicating a "soft" shear mode in the *XY* plane. The Born stability criteria were evaluated, and their fulfillment confirms the thermodynamic stability of the crystal. The Cauchy relations were also analyzed. The spatial distributions of Young's modulus and Poisson's ratio of K_2SO_4 crystals were constructed. The Young's modulus surface is close to spherical in shape (a "rounded parallelepiped") with pronounced protrusions along the [010] and [001] crystallographic directions. The values of Poisson's ratio (within 0.23–0.27) are typical for ionic-covalent crystals of intermediate stiffness, indicating moderate transverse deformation. The elasto-optic parameters of K_2SO_4 crystals were analyzed. The baric (pressure-induced) changes in the refractive indices were calculated. It is shown that the temperature variation of the refractive index (dn_i / dT) in these crystals is governed by a complex interplay between volumetric and structural factors. The contributions to the temperature-induced refractive index changes arising from variations in atomic polarizability (≈ 32%) and crystal density (≈ 68%) were estimated.

Keywords: crystal, elastic stiffness coefficients, Born criterion, Poisson's ratio, Young's modulus, refractive index.

1. Introduction

Most physical, mechanical, and optical properties of real crystalline materials are anisotropic, i.e., they strongly depend on the measurement direction with respect to the crystallographic axes. The anisotropy of the refractive index, birefringence, photoelastic, and acousto-optic responses is a direct consequence of the anisotropic distribution of interatomic forces and electronic polarizability within the crystal lattice. Understanding the relationship between the elastic and optical properties of anisotropic materials is a key objective of modern solid-state physics, crystal optics, and materials science.

Photoelasticity represents one of the fundamental mechanisms coupling the elastic and optical properties of crystals. Lattice deformation induced by external stresses or acoustic waves leads to changes in the dielectric permittivity tensor and, consequently, to modulation of the refractive index and birefringence.

Particular interest is attracted to anisotropic crystals with a high acousto-optic figure of merit, in which an optimal combination of elastic, optical, and elasto-optic parameters ensures efficient diffraction of light by acoustic waves. The anisotropy of elastic moduli and refractive indices makes it possible to realize interaction geometries that provide maximum values of the acousto-optic figure of merit. This opens broad prospects for the development of highly efficient acousto-optic modulators, deflectors, and filters for laser beam control over a wide spectral range.

Beyond their practical relevance, investigations of optical and photoelastic anisotropy are of fundamental importance, as they enable a deeper understanding of the nature of interatomic forces, the role of electronic polarizability, and the anharmonicity of lattice vibrations. Temperature- and strain-induced changes in birefringence and refractive indices serve as sensitive indicators of structural rearrangements and phase transitions in crystals.

Thus, the anisotropy of elastic, optical, and photoelastic properties is a key factor in the rational design of functional materials for crystal optics and acousto-optics, particularly for the development of light-control elements based on anisotropic ionic crystals [1–9].

The K_2SO_4 crystal was chosen as the object of investigation. It exhibits two polymorphic modifications: β-K_2SO_4 below 587 °C and α-K_2SO_4 at higher temperatures. The crystal lattice of α-K_2SO_4 is described in the hexagonal setting with lattice parameters $a = 5.90$ (2) Å and $c = 8.11$ (3) Å [10, 11] and belongs to the space group $P6_3/mmc$. The α-K_2SO_4 structure is dynamically disordered, being characterized by orientational disorder of the SO_4^{2-} groups [12] and restricted rotational freedom [13]. The β-K_2SO_4 phase (below 587 °C) contains four formula units per unit cell with lattice parameters $a = 0.5731$ nm, $b = 1.008$ nm, and $c = 0.7424$ nm [14]. The c axis is pseudo-hexagonal. In potassium sulfate crystals, the SO_4^{2-} group forms a rigid tetrahedron with the sulfur ion located at the center and oxygen ions at the vertices; the sulfur and potassium ions, together with two oxygen ions from each SO_4^{2-} tetrahedron, lie in two parallel planes. The β-K_2SO_4 structure is orthorhombic (pseudo-hexagonal) and belongs to the space group D_{2h}^{16}–$Pnam$.

Previously, a series of investigations of the refractive parameters of K_2SO_4 crystals has been carried out. In particular, the influence of uniaxial mechanical stresses on the spectral (300–800 nm) and temperature (77–700 K) dependences of the refractive indices n_i and birefringence Δn_i was experimentally studied, and their anomalous behavior in the vicinity of phase transitions was revealed [15, 16].

The baric variations of the parameters of the Sellmeier equation, electronic polarizability, and refractivities of K_2SO_4 crystals were calculated. The electronic band structure and density of states were determined, and the band gap energy of K_2SO_4 crystals was evaluated [17–19]. However, a comprehensive study of the elastic and elasto-optic parameters has not yet been performed.

The aim of the present work is to calculate the elastic stiffness matrix of the K_2SO_4 crystal, to analyze the character of its anisotropy, and to compare the obtained results with the anisotropy of the optical parameters.

2. Calculation method

The elastic properties of K_2SO_4 crystals were calculated using the CASTEP code, which is based on density functional theory [20, 21]. The following valence electron configurations were employed: O $2s^2\ 2p^4$; S $3s^2\ 3p^4$; K $3s^2\ 3p^6\ 4s^1$. The ionic cores were described using norm-conserving pseudopotentials [22]. Integration over the first Brillouin zone was performed using a $3 \times 2 \times 4$ k-point mesh. Exchange-correlation effects were accounted for within the local density approximation for crystal structure optimization, as it provides better agreement with experimental lattice parameters [23]. Calculations of elasto-optic and electronic properties were performed using the generalized gradient approximation with the Perdew–Burke–Ernzerhof parameterization to ensure a more accurate description of electron density gradients [24–26].

The structural optimization procedure was carried out similarly to Refs. 27, 28 with the following convergence criteria: maximum force $3 \cdot 10^{-2}$ eV/Å, maximum stress $5 \cdot 10^{-3}$ GPa, and maximum atomic displacement $1 \cdot 10^{-4}$ Å.

The crystallographic data reported in Refs. 15, 16 were used as input for the elastic property calculations. The corresponding structure belongs to the space group No. 62 (*Pnma*). Prior to the elastic calculations, the crystal structure was fully optimized within the chosen computational approach. The experimental and optimized x, y, and z atomic coordinates for the K_2SO_4 crystal are summarized in Table 1 [29].

Table 1. Experimental and optimized x, y, and z atomic coordinates for the β-K_2SO_4 crystal (D is the estimated standard deviation) [29]

Atom	Experimental coordinates			Optimized coordinates			D
	x	y	z	x	y	z	
O	2.24953	0.23744	3.54701	2.28232	0.24504	3.64214	0.10091
O	1.48847	–0.23744	–1.48849	1.53303	–0.24504	–1.50831	0.04936
O	–2.24953	–2.64406	–3.54701	–2.28232	–2.69625	–3.64214	0.11335
O	–1.48847	2.64406	1.48849	–1.53303	2.69625	1.50831	0.07143
O	–2.24953	–0.23744	–3.54701	–2.28232	–0.24504	–3.4214	0.10091
O	–1.48847	0.23744	1.48849	–1.53303	0.24504	1.50831	0.04936
O	2.24953	2.64406	3.54701	2.28232	2.69625	3.64214	0.11335
O	1.48847	–2.64406	–1.48849	1.53303	–2.69625	–1.50831	0.07143
O	0.28334	1.44075	4.19558	0.27358	1.47064	4.30905	0.11775
O	2.21514	1.44075	–4.44937	2.25872	1.47064	–4.54622	0.11033
O	3.45466	–1.44075	–0.83992	3.54177	–1.47064	–0.8414	0.09211
O	1.52286	–1.44075	0.58613	1.55663	–1.47064	0.60423	0.04859
O	–0.28334	–1.44075	–4.19558	–0.27358	–1.47064	–4.30905	0.11775
O	–2.21514	–1.44075	4.44937	–2.25872	–1.47064	4.54622	0.11033

Table 1 (continued)

Atom	Experimental coordinates			Optimized coordinates			*D*
	x	*y*	*z*	*x*	*y*	*z*	
O	–3.45466	1.44075	0.83992	–3.54177	1.47064	0.8414	0.09211
O	–1.52286	1.44075	–0.58613	–1.55663	1.47064	–0.60423	0.04859
S	1.74176	1.44075	4.2269	1.76254	1.47064	4.33492	0.11399
S	1.99624	–1.44075	–0.8086	2.05281	–1.47064	–0.81552	0.06435
S	–1.74176	–1.44075	–4.2269	–1.76254	–1.47064	–4.33492	0.11399
S	–1.99624	1.44075	0.8086	–2.05281	1.47064	0.81552	0.06435
K	–2.4389	1.44075	4.13535	–2.46494	1.47064	4.26191	0.13262
K	–0.08254	1.44075	–2.98041	–0.06607	1.47064	–3.06482	0.09105
K	–1.2991	–1.44075	–0.90015	–1.3504	–1.47064	–0.88853	0.0605
K	–3.65546	–1.44075	2.05509	–3.74928	–1.47064	2.08562	0.10309
K	2.4389	–1.44075	-4.13535	2.46494	–1.47064	–4.26191	0.13262
K	0.08254	–1.44075	2.98041	0.06607	–1.47064	3.06482	0.09105
K	1.2991	1.44075	0.90015	1.3504	1.47064	0.88853	0.0605
K	3.65546	1.44075	–2.05509	3.74928	1.47064	–2.08562	0.10309

The investigation of elastic properties is of considerable importance, as they are directly related to sound velocities, heat transport, mechanical characteristics, and other physical parameters. Elastic properties are described by Hooke's law, which for anisotropic materials can be written in the following form [1, 30]:

$$\sigma_{mk} = C_{mknl}\delta_{nl}, \quad (1)$$

where σ_{mk} is the mechanical stress tensor, C_{mknl} are the elastic stiffness constants, and δ_{nl} is the strain tensor. The K_2SO_4 crystal belongs to the orthorhombic symmetry class; therefore, its elastic constants form a symmetric 6 × 6 matrix. This matrix contains 12 nonzero components, nine of which are independent: C_{11}, C_{22}, C_{33}, C_{44}, C_{55}, C_{66}, C_{12}, C_{13}, and C_{23}.

The elastic coefficients C_{ij} were obtained by expanding the total energy $E(V, \delta)$ of the crystal in a Taylor series with respect to the unit cell volume V and strain δ. For small deformations ($\delta \ll 1$), the energy per unit volume is expressed as follows [1, 31]:

$$E(V,\delta) = E(V_0,0) + V_0\sum_{i=1}^{6}\sigma_i e_i + \frac{V_0}{2}\sum_{i,j=1}^{6}C_{ij}e_i e_j + \ldots \quad (2)$$

Here, V_0 denotes the equilibrium volume at zero pressure, e_i are the components of the strain tensor in Voigt notation, and C_{ij} are the second-order elastic stiffness coefficients, defined as the curvature of the energy surface:

$$C_{ij} = \frac{1}{V_0}\left[\frac{\partial^2 E}{\partial e_i \partial e_j}\right]. \quad (3)$$

To determine all nine independent elastic coefficients, a set of strain tensors was applied. Each strain δ induces a change in the total energy, $\Delta E = E(\delta) - E(0)$, which is a quadratic function of δ. For the calculation of the longitudinal and transverse elastic constants (C_{11}, C_{22}, C_{33}, C_{12}, C_{13}, C_{23}), uniaxial tensile/compressive strains along the crystallographic axes were applied.

For example, for a deformation along the *X* axis: δ = (δ, 0, 0, 0, 0, 0)

$$\Delta E / V_0 = \frac{1}{2}C_{11}\delta^2. \quad (4)$$

Taking into account the calculated values of C_{11} and C_{22}, the coefficient C_{12} was subsequently determined. To evaluate the shear moduli (C_{44}, C_{55}, C_{66}), volume-conserving shear strains (up to higher-order terms) were applied. For a shear deformation in the *YZ* plane [ε = (0, 0, 0, δ, 0, 0) in Voigt notation], the corresponding energy variation can be written as:

$$\Delta E / V_0 = \frac{1}{2}C_{44}\delta^2. \quad (5)$$

Similarly, C_{55} was determined from a shear deformation in the *XZ* plane, and C_{66} from a shear deformation in the *XY* plane.

3. Results and discussion

3.1. Elastic properties of K_2SO_4 *crystals*

Table 2 presents the calculated elastic stiffness matrix C_{ij} (GPa) of K_2SO_4 at room temperature. The matrix contains 9 independent components, which is characteristic of orthorhombic crystals. All other components are zero. Table 3 lists the experimental values of the elastic constants C_{ij} (GPa) for the same crystal [31].

Comparison of the theoretical and experimental data allows us to evaluation of the accuracy of calculations. The experimental values of C_{11}, C_{22}, and C_{33} are approximately 5% higher than the theoretical ones, indicating that the real crystal is slightly "stiffer" than predicted by the model in Table 3.

Table 2. Calculated elastic stiffness matrix C_{ij} (GPa) of K_2SO_4 at room temperature

51.07	18.12	20.01	0	0	0
18.12	51.13	18.90	0	0	0
20.01	18.90	52.03	0	0	0
0	0	0	17.21	0	0
0	0	0	0	14.11	0
0	0	0	0	0	13.41

In both cases, the C_{66} coefficient is the smallest among the diagonal elements, indicating a "soft" shear mode in the *XY* plane.

The mechanical stability of the crystal was evaluated using the Born criteria, which require the strain energy density to be positive definite. For the studied system, the diagonal elements satisfy $C_{11} \approx C_{22} \approx C_{33} > C_{44} > C_{55} > C_{66}$, indicating nearly isotropic longitudinal stiffness along the principal crystallographic axes combined with a pronounced anisotropy of shear resistance. Stability is further confirmed by the positive values of the successive principal minors: the first-order minor ($C_{11} > 0$), the second-order minor ($C_{11}C_{22} - C_{12}^2 = 2282.9 > 0$), and the third-order minor:

$$C_{11}C_{22}C_{33} + 2C_{12}C_{13}C_{23} - C_{11}C_{23}^2 - C_{22}C_{13}^2 - C_{33}C_{12}^2 > 0.$$

As shown in Table 2, the diagonal shear components C_{44}, C_{55}, and C_{66} are also greater than zero; thus, the Born criteria are satisfied, and the crystal structure is thermodynamically stable.

The Cauchy relations state that if the interatomic forces are purely central and every atom occupies a center of inversion, the following equalities must hold:

$$C_{12} = C_{66},\ C_{13} = C_{55},\ C_{23} = C_{44}. \quad (6)$$

Table 2 shows that $C_{12} \neq C_{66}$ (discrepancy $\Delta = 4.71$), $C_{13} \neq C_{55}$ ($\Delta = 5.90$), and $C_{23} \neq C_{44}$ ($\Delta = 1.69$). In the K_2SO_4 crystal, the inequality of the $C_{ij} \neq C_{kl}$ coefficients indicates the presence of significant non-central forces (covalent contribution or many-body interactions). The deviation from the Cauchy relations suggests that the interaction potential depends not only on distance but also on the bond angles.

Thus, the K_2SO_4 crystal satisfies the Born stability criteria, confirming the stability of its orthorhombic phase. The violation of the Cauchy relations (particularly $C_{13} \neq C_{55}$) indicates the dominance of non-central interatomic forces. The theoretical values of the elastic constants (Table 2) are slightly lower (by 3–5 GPa) than the experimental data; however, they accurately represent the overall elastic anisotropy of the crystal.

Since the K_2SO_4 crystal possesses orthorhombic symmetry, its elastic properties are highly direction-dependent. To calculate Young's modulus (E) and Poisson's ratio (ν), the stiffness matrix (Table 2) must first be inverted to obtain the compliance matrix $S = C^{-1}$. Here, it is taken into account that the principal Young's moduli for the orthorhombic system are defined by the diagonal components of the compliance matrix $E_x = 1/S_{11}$, $E_y = 1/S_{22}$, $E_z = 1/S_{33}$. The compliance matrix S_{ij} and the stiffness matrix C_{ij} are mutually inverse. All calculations were based on the previously obtained experimental data listed in the table and cited accordingly. For an orthorhombic system, the principal Young's moduli along the main axes [100], [010], and [001] are defined as $E_i = S_{ii}^{-1}$. Using the experimental data (Table 3), we obtain E_x (E_{11}) ≈ 42.5 GPa, E_y (E_{22}) ≈ 45.9 GPa, E_z (E_{33}) ≈ 44.0 GPa.

Young's modulus in an arbitrary direction, defined by a unit vector **n** (l_1, l_2, l_3), where l_i are the direction cosines, is calculated using the following formula:

$$E^{-1} = l_1^4 S_{11} + l_2^4 S_{22} + l_3^4 S_{33}$$

$$+ l_2^2 l_3^2 (2S_{23} + S_{44}) + l_1^2 l_3^2 (2S_{13} + S_{55}) + l_1^2 l_{23}^2 (2S_{12} + S_{66}). \quad (7)$$

Poisson's ratio defines the ratio of relative transverse strain to longitudinal strain. For the principal axes, the Poisson's ratios are given by

$$\nu_{ij} = -S_{ij} / S_{ii}. \quad (8)$$

Here, $\nu_{12} \approx 0.23$ (compression along *X*, strain along *Y*); $\nu_{13} \approx 0.27$ (compression along *X*, strain along *Z*); and $\nu_{23} \approx 0.25$ (compression along *Y*, strain along *Z*).

Figure 1 illustrates the spatial anisotropy of Young's modulus (E) and Poisson's ratio (ν) for the K_2SO_4 crystal. It can be observed that the Young's modulus surface exhibits a shape close to spherical (a "rounded parallelepiped"), where the radius vector to the surface is proportional to the modulus value in that direction. Notable "protrusions" are detected along the [010] (*b*-axis) and [001] (*c*-axis) directions. This indicates that the crystal is least compressible specifically along these axes. This surface demonstrates how the crystal stiffness varies during tension along the vector **n**. Since the coefficient C_{66} = 14.24 GPa is significantly lower than the other shear moduli, the crystal exhibits the highest shear compliance in the (001) plane.

The values of the Poisson's ratio (0.23–0.27) are typical for ionic-covalent crystals of moderate stiffness, indicating moderate transverse deformation. The crystal exhibits orthotropic anisotropy, where the *XY* plane is the most compliant

Table 3. Experimentally measured values of elastic stiffness matrix C_{ij} (GPa) of K_2SO_4 at room temperature [31]

C_{11}	C_{12}	C_{13}	C_{22}	C_{23}	C_{33}	C_{44}	C_{55}	C_{66}
53.57	19.99	20.95	56.53	19.90	55.23	19.23	18.79	14.24

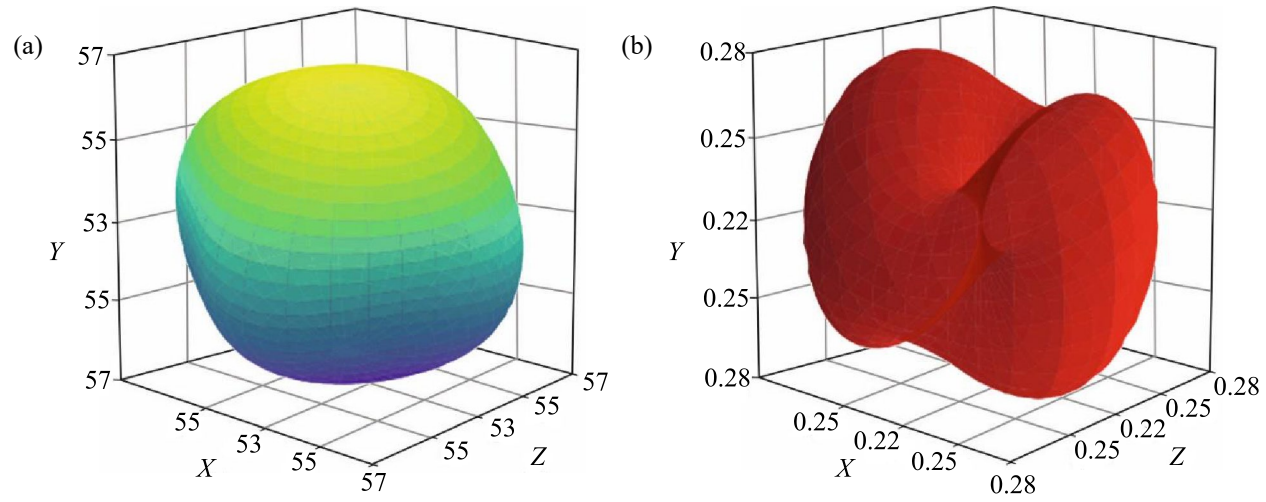

Fig. 1. Spatial anisotropy of the Young's modulus E (a) and the Poisson's ratio (b) for the K_2SO_4 crystal.

direction for shear, correlating with the lowest elastic coefficient value. The absence of negative values indicates that the K_2SO_4 crystal is not auxetic. That is, under tension along the applied force, the crystal elongates while contracting in the perpendicular direction, which represents standard "normal" mechanical behavior. It is also observed that the Young's modulus fluctuates between 42.5 and 45.9 GPa depending on the direction, reaching its maximum along the [010] axis. The Poisson's ratio is more complex, as it depends not only on the tensile direction **n**, but also on the direction in which the transverse strain is measured **m** (**n** ⊥ **m**):

$$\nu(n,m) = -E(n) S_{ijkl} n_i n_j m_l m_k \,. \tag{9}$$

To construct the three-dimensional surface, either the maximum value $\nu_{max}(n)$ for each direction or the average value is typically used. It can be observed that the maximum values of E occur along the crystallographic axes (the vertices of the surface), which is characteristic of systems with high ionic density. The lowest stiffness is observed at an angle of 45° to the axes, where the contribution of the shear components (S_{44}, S_{55}, and S_{66}) becomes dominant.

The Poisson's ratio for the K_2SO_4 crystal is non-isotropic [Fig.1(b)]. The "indentations" (or dips) in the surface indicate directions where the crystal is difficult to compress laterally under tension. If the Cauchy relations were satisfied, these surfaces would exhibit higher symmetry. The deviations observed (asymmetry of the lobes) confirm the presence of non-central forces in the potassium sulfate lattice.

Thus, the spatial distribution of the Young's modulus for the K_2SO_4 crystal demonstrates orthotropic symmetry, with maxima along the [100], [010], and [001] axes (42.5, 45.9, and 44.0 GPa, respectively). The red surface of the Poisson's ratio visualizes the anisotropy of transverse contraction; it possesses a complex lobed shape, where the highest values are reached in planes parallel to the axes with the lowest C_{ij} values (the XY plane, due to the low value of C_{66}).

Using the obtained C_{ij} matrices, the bulk modulus (B) was calculated using the following relationship:

$$B = \frac{1}{9}\left[C_{11} + C_{22} + C_{33} + 2\left(C_{12} + C_{13} + C_{23}\right)\right] = 29.81 \text{ GPa}, \tag{10}$$

as well as the shear modulus (G = 17.15 GPa).

The observed behavior of the elastic coefficients in the K_2SO_4 crystal is attributed to the presence of rigid tetrahedral SO_4^{2-} groups. The bonding within these groups is covalent, implying the presence of directional bonds. Unlike ionic bonding, which acts isotropically in all directions, directional bonds provide resistance not only to changes in interatomic distances but also to changes in the bond angles.

It is also evident from the matrix that the Cauchy parameter $g = (C_{12} - C_{44}) = 0.91$ GPa is positive, which indicates a predominant ionic character with pronounced polarizability. This is a consequence of the interatomic forces "maintaining" the structure through both electrostatic attraction and the rigid geometry of the sulfate groups.

Thus, the complex nature of the forces in the K_2SO_4 crystal arises because the lattice is composed of polarizable ions and molecular SO_4^{2-} complexes with internal covalent bonding, rather than simple point charges. This results in the material being elastically anisotropic and highly sensitive to the direction of the applied load.

3.2. Photorefractive properties of potassium sulfate crystals

It is well known that photoelasticity defines the change in the optical indicatrix under the influence of mechanical stress, and it is expressed as follows [32, 33]:

$$\Delta\left(\frac{1}{n_i^2}\right) = p_{ij}\varepsilon_j, \tag{11}$$

where p_{ij} are the photoelastic coefficients (or elasto-optic coefficients), n_i are the refractive indices, and ε_j are the

strain components. For small baric (hydrostatic) changes, the relationship is written as:

$$\frac{dn_i}{dp} = -\frac{n_i^3}{2}\sum_j p_{ij}\frac{d\varepsilon_j}{dp}. \quad (12)$$

Since

$$\frac{d\varepsilon_j}{dp} = -\left[S_{j1} + S_{j2} + S_{j3}\right], \quad (13)$$

the following relationship can be obtained:

$$\frac{dn_i}{dp} = -\frac{n_i^3}{2}\sum_j p_{ij}\left[S_{j1} + S_{j2} + S_{j3}\right]. \quad (14)$$

According to Eq. (14), the baric change in the refractive index dn_i/dp depends not only on the elastic compliance matrix components S_{ij} but also explicitly on the refractive index n_i and the elasto-optic coefficients p_{ij}. The reciprocal bulk modulus $1/B$ for the crystal under study is determined by Eq. (10). At the same time, in Eq. (14), the corresponding compliance components enter with weighting factors p_{ij} and are multiplied by the factor $n_i^3/2$. Introducing the effective hydrostatic elasto-optic coefficient p_i^{eff}, we obtain

$$\frac{dn_i}{dp} = -\frac{n_i^3}{2}p_{ij}^{\text{eff}}\frac{1}{B}. \quad (15)$$

This expression allows one to estimate the effective values of the elasto-optic coefficients from the experimentally obtained refractive indices, their pressure-induced variations, and the calculated values of B. This, in turn, will enable the assessment of the acousto-optic properties of the studied crystals, which is crucial for the development of acousto-optic modulators and deflectors to control electromagnetic radiation. Such research is planned for the future.

We obtained a value of $B \approx 30$ GPa (1 GPa = 10^4 bar), which yields $1/B \approx 3.3\cdot10^{-6}$ bar^{-1}, consistent with previously reported values. Since $S_{11} \neq S_{22} \neq S_{33}$, the photoelastic effect differs for the refractive indices n_x, n_y, n_z. That is, $\frac{dn_x}{dp} \neq \frac{dn_y}{dp} \neq \frac{dn_z}{dp}$, and their anisotropy is determined by the anisotropic part of the compliance matrix S_{ij}.

The temperature dependence of the crystal's refractive index $n_i(T)$ is also related to its elastic properties, as temperature changes induce changes in volume and, consequently, the material density, which is a manifestation of its elastic response. Furthermore, temperature influences the electronic polarizability of atoms and ions.

The temperature dependence of the refractive index can be expressed as follows:

$$\left(dn/dT\right) = \left(\partial n/\partial T\right)_\rho + \left(\partial n/\partial \rho\right)_T\left(d\rho/dT\right). \quad (16)$$

The first term describes the changes in electronic polarizability associated with anharmonicity and the reorientation of structural elements. Temperature affects the electron shells of atoms, altering their deformability in an electric field (i.e., their polarizability). This effect is typically smaller than the volumetric contribution but can be significant in certain materials. The second term describes the impact of thermal expansion (change in the crystal density, ρ). As the crystal temperature rises, atoms vibrate with greater amplitude, leading to an increase in the average interatomic distance and a corresponding volumetric expansion. This reduces the number of oscillators (atoms/molecules) per unit volume, which generally results in a decrease in the refractive index. This effect is a direct manifestation of the material's elastic properties.

Internal deformation processes, induced by the lattice vibration anharmonicity, influence the electronic polarizability α_e. Anharmonicity leads to a temperature-induced shift of the energy bands (a decrease in the band gap E_g). This increases the electronic polarizability, providing a positive contribution to dn/dT. If the contribution from the polarizability change (due to anharmonicity) exceeds that of thermal expansion, the refractive index increases with temperature (as seen in semiconductors). Conversely, if expansion dominates, the index decreases (typical for ionic crystals).

Using the calculated value of $\partial n/\partial\rho \approx 1\cdot10^{-4}$ m^3/kg [34], along with previously obtained values for the thermo-optic coefficients ($dn_i/dT \approx 4\cdot10^{-5}$ K^{-1}) and linear expansion [$(\Delta l/l_0)_i \approx 3\cdot10^{-5}$] [35], we have estimated the contributions to the thermal changes in the refractive indices: approximately from the change in atomic polarizability (≈ 32%) and from the change in crystal density (≈ 68%). Previously, similar relationships between the temperature and pressure variations of refractive indices were observed for isomorphic crystals $(NH_4)_2SO_4$, $RbKSO_4$, Rb_2SO_4 and $(NH_4)_2BeF_4$ [36–39].

Thus, the thermal variation of n_i in orthorhombic crystals results from the competition between thermal expansion (which decreases n_i) and the anharmonic increase in polarizability (which increases n_i); in the orthorhombic system, both effects exhibit different magnitudes along the three principal axes.

Conclusions

In this work, the elastic constants of K_2SO_4 crystals were calculated at room temperature. The obtained values are slightly lower than the experimental data (by approximately 5%). Among the diagonal elements, C_{66} is the smallest, indicating a "soft" shear mode in the plane XY.

The Born stability criteria were satisfied, confirming the thermodynamic stability of the crystal. Furthermore, the analysis of the Cauchy relations showed significant deviations ($C_{ij} \neq C_{kl}$), indicating the presence of substantial non-central forces, such as covalent contributions or many-body interactions.

The spatial distributions of Young's modulus and Poisson's ratio for the K_2SO_4 crystal were constructed.

The Young's modulus surface exhibits a shape close to a "rounded parallelepiped" with distinct protrusions along the [010] (*b*-axis) and [001] (*c*-axis) directions, identifying these as the directions of minimum compressibility. The Poisson's ratio values (ranging from 0.23 to 0.27) are typical for ionic-covalent crystals of moderate stiffness, indicating moderate transverse deformation. The absence of negative values confirms that the crystal is not an auxetic.

The photoelastic (elasto-optic) parameters of K_2SO_4 crystals were analyzed. Using the calculated bulk modulus, the baric (pressure-induced) changes in the refractive indices were determined.

It was demonstrated that the thermo-optic coefficient dn_i/dT is governed by a complex interplay of volumetric and structural factors. The thermal variation of the refractive indices in K_2SO_4 crystals results from the competition between thermal expansion (which decreases n_i) and the anharmonic increase in polarizability (which increases n_i). In the orthorhombic system, both effects exhibit different magnitudes along the three principal axes. The contribution to the temperature-induced changes in the indices was estimated to be approximately 32% from the change in atomic polarizability and 68% from the change in crystal density.

Acknowledgments

The study was carried out within the framework of the state budget topic "Structural and functional studies of A_2BX_4 materials for sensors and dual-purpose electromagnetic radiation control devices" (No. 0126U002474).

1. J. F. Nye, *Physical Properties of Crystals*: *Their Representation by Tensors*, Oxford University, Clarendon Press (1985).
2. T. C. T. Ting, *Anisotropic Elasticity*: *Theory and Applications*, Oxford University, Clarendon Press (1996).
3. R. E. Newnham, *Properties of Materials*: *Anisotropy*, *Symmetry*, *Structure*, Oxford University, Clarendon Press (2004).
4. R. M. Waxler and A. Feldman, *Appl. Optic Eng.* **19**, 2481 (1980).
5. B. Mytsyk, *Ukr. J. Phys. Opt.* **4**, 105 (2003).
6. S. Oseledchik, A. Prosvirnin, A. I. Pisarevskiy *et. al.*, *Opt. Mater.* **4**, 669 (1995).
7. A. Polian and M. Grimsditch, *Phys. Rev. B* **60**, 1468 (1999).
8. E. Chilla, C. M. Flannery, H.-J. Frohlich, and U. Straube, *J. Appl. Phys.* **90**, 6084 (2001).
9. N. Zhang, J. Wu, and H. Zhang, *Crystals* **15**, 269 (2025).
10. H. Arnold, W. Kurtz, A. Richter-Zinnius, and J. Bethke, *Acta Cryst. B* **37**, 1643 (1981).
11. M. Miyake and S. Iwai, *Phys. Chem. Mater.* **7**, 211 (1981).
12. S. Shiozaki, A. Sawada, and J. Ishibashi, *J. Phys. Soc. Jpn.* **43**, 1314 (1977).
13. F. A. I. El-Kabbany, *Phys. Status Solidi A* **58**, 373 (1980).
14. A. I. Berg and H. Tuinstra, *Acta Cryst. B* **34**, 3177 (1978).
15. B. Andriyevsky, M. Jaskólski, V. Stadnyk, M. Romanyuk, and O. Kashuba, *Comp. Mater. Sci.* **79**, 442 (2013).
16. B. Andriyevsky, M. Romanyuk, and V. Stadnyk, *J. Phys. Chem. Sol.* **70**, 1109 (2009).
17. V. Yo. Stadnyk, M. O. Romanyuk, O. Z. Chyzh, and V. F. Vachulovych, *Condens. Matter Phys.* **10**, 45 (2007).
18. V. M. Gaba, V. Y. Stadnyk, O. S. Kushnir, and O. Z. Chizh, *Opt. Spectr.* **110**, 967 (2011).
19. V. Y. Stadnyk, O. S. Kushnir, R. S. Brezvin, and V. M. Gaba, *Opt. Spectr.* **106**, 614 (2009).
20. S. J. Clark, M. D. Segall, C. J. Pickard, P. J. Hasnip, M. I. J. Probert, K. Refson, and M. C. Payne, *Zeitschrift für Kristallographie – Crystalline Materials* **220**, Issue 5–6, 567 (2005).
21. P. Hohenberg and W. Kohn, *Phys. Rev.* **136**, B864 (1964).
22. W. Kohn and L. J. Sham, *Phys. Rev.* **140**, A1133 (1965).
23. C. Lee, W. Yang, and R. G. Parr, *Phys. Rev. B* **37**, 785 (1988).
24. P. J. Stephens, F. J. Devlin, C. F. Chabalowski, and M. J. Frisch, *J. Phys. Chem.* **98**, 11623 (1994).
25. J. P. Perdew, K. Burke, and M. Ernzerhof, *Phys. Rev. Lett.* **77**, 3865 (1996).
26. J. P. Perdew and A. Zunger, *Phys. Rev. B* **23**, 5048 (1981).
27. W. Kraus and G. Nolze, *J. Appl. Cryst.* **29**, 301 (1996).
28. *The Rietveld Method*, R. A. Young (ed.), IUCr Monographs of Crystallography, Oxford University Press (1993).
29. J. A. McGinnety, *Acta Cryst. B* **28**, 2845 (1972).
30. T. S. Narasimhamurty, *Photoelastic and Electro-Optic Properties of Crystals*, New York and London, Plenum Press (1981).
31. Von S. Haussühl, *Acta Cryst.* **18**, 839 (1965).
32. M. O. Romanyuk, *Crystal Optics*, Lviv, Ivan Franko LNU Press (2017).
33. B. G. Mytsyk, *The Photoelasticity of Anisotropy Materials*, Lviv, Liga-Press (2012).
34. V. Yo. Stadnyk, M. O. Romanyuk, O. Z. Chyzh, and V. F. Vachulovych, *Condens. Matter Phys.* **10**, 45 (2007).
35. R. S. Brezvin, V. M. Gaba, M. O. Romanyuk, and V. Y. Stadnyk, *Optoelectronic Parameters of Ferroics of the Sulfate and Zincate Groups*, Lviv, Liga-Press (2018).
36. B. Mytsyk, V. Stadnyk, N. Demyanyshyn, Y. Kost, and P. Shchepanskyi, *Opt. Mater.* **88**, 723 (2019).
37. V. Yo. Stadnyk, N. A. Romanyuk, and R. S. Brezvin, *Crystal. Rep.* **50**, 961 (2005).
38. I. A. Pryshko, I. S. Novosad, Z. O. Kohut, V. M. Salapak, and O. M. Horina, *Low Temp. Phys.* **50**, 584 (2024) [*Fiz. Nyzk. Temp.* **50**, 649 (2024)].
39. V. Y. Stadnyk and M. O. Romanyuk, *Phys. Status Solidi A* **158**, 289 (1996).

Пружно-оптичні параметри кристалів K_2SO_4

O. A. Markevych, O. M. Horina, V. Y. Stadnyk, R. S. Brezvin, Z. O. Kohut, I. B. Pirko

Розраховано коефіцієнти пружної жорсткості кристалів K_2SO_4 за кімнатної температури. Коефіцієнт C_{66} є найменшим

серед діагональних компонент, що вказує на наявність «м'якої» моди зсуву в площині *XY*. Оцінено критерії стійкості Борна; їх виконання підтверджує термодинамічну стабільність кристала. Також проаналізовано співвідношення Коші. Побудовано просторові розподіли модуля Юнга та коефіцієнта Пуассона кристалів K_2SO_4. Поверхня модуля Юнга за формою близька до сферичної («заокруглений паралелепіпед») із вираженими виступами вздовж кристалографічних напрямків [010] і [001]. Значення коефіцієнта Пуассона (у межах 0,23–0,27) є типовими для іонно-ковалентних кристалів проміжної жорсткості, що вказує на помірну поперечну деформацію. Проаналізовано пружно-оптичні параметри кристалів K_2SO_4. Розраховано баричні (зумовлені тиском) зміни показників заломлення. Показано, що температурна зміна показника заломлення (dn_i / dT) у цих кристалах визначається складною взаємодією об'ємних та структурних факторів. Оцінено внески в температурні зміни показника заломлення, що виникають внаслідок зміни атомної поляризовності (≈ 32%) та густини кристала (≈ 68%).

Ключові слова: кристал, коефіцієнти пружної жорсткості, критерій Борна, співвідношення Пуассона, модуль Юнга, показник заломлення.